Supporting Information for "Critical Role of External Axial Ligands in Chirality Amplification of *trans*-Cyclohexane-1,2-diamine in Salen Complexes"

Takuya Kurahashi,[†] Masahiko Hada[‡] and Hiroshi Fujii[*,†]

Institute for Molecular Science & Okazaki Institute for Integrative Bioscience, National Institutes of Natural Sciences, Myodaiji, Okazaki, Aichi 444-8787, Japan and Department of Chemistry, Graduate School of Science, Tokyo Metropolitan University, 1-1 Minami-Osawa, Hachioji-shi, Tokyo 192-0397, Japan

* To whom correspondence should be addressed. E-mail: hiro@ims.ac.jp

[†] National Institutes of Natural Sciences

[‡] Tokyo Metropolitan University

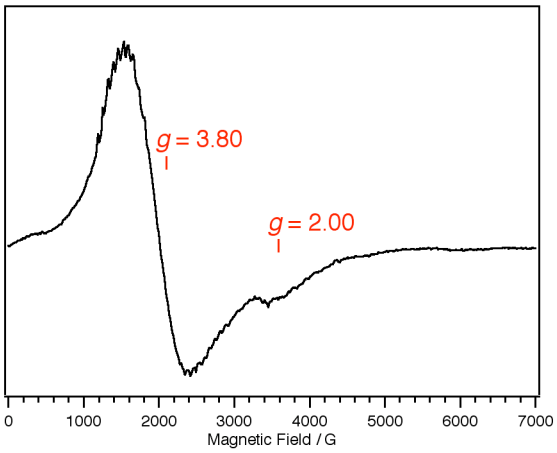

Figure S1. X-band EPR spectra of **2**-N_3 in frozen CH_2Cl_2 at 4 K. Magnetic parameters: $E/D \approx 0$. Conditions: microwave frequency, 9.56 GHz; microwave power, 2.012 mW; modulation amplitude, 7 G; time constant, 163.84 ms; conversion time, 163.84 ms.

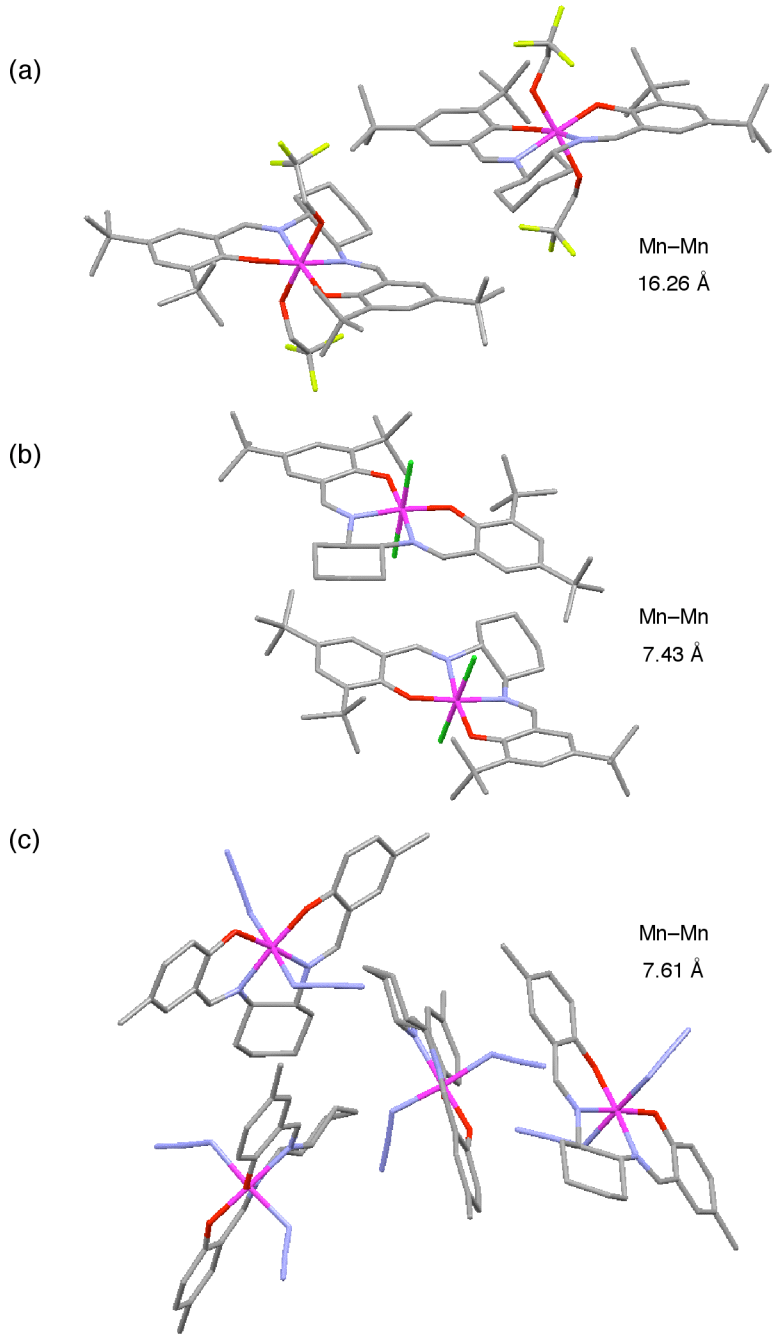

Figure S2. Packing diagrams for (a) **1**-OCH_2CF_3, (b) **1**-Cl and (c) **2**-N_3. Hydrogen atoms and non-coordinated solvent molecules are omitted for the sake of clarity.

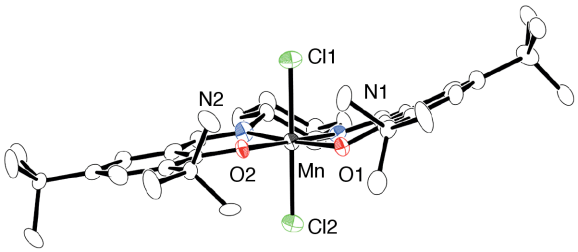

Figure S3. X-ray crystal structure of one of two **1**-Cl molecules that are contained in the asymmetric unit. The other molecule is shown in Figure 3a. Thermal ellipsoids represent the 50% probability surfaces. Hydrogen atoms are omitted for the sake of clarity.

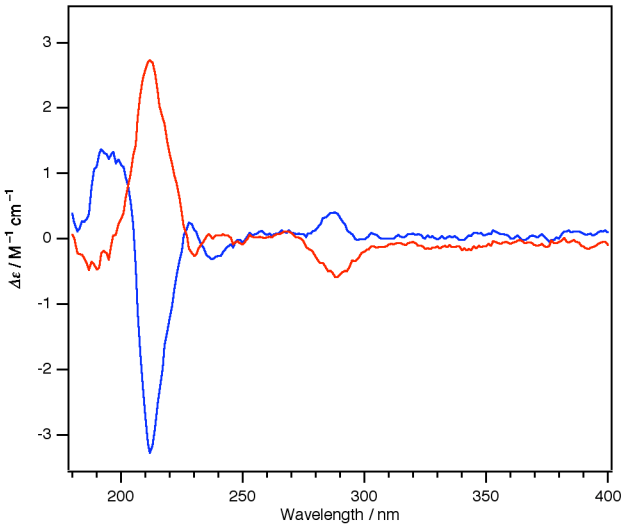

Figure S4. Circular dichroism spectra of (*R*,*R*)-**3** (red line) and (*S*,*S*)-**3** (blue line) in CH_3CN (0.3 mM) at room temperature.

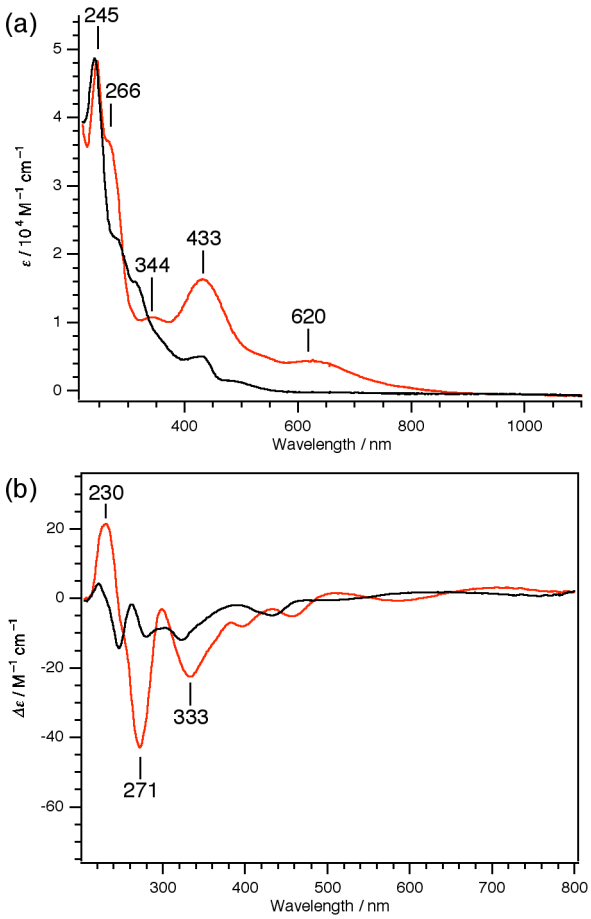

Figure S5. (a) UV-vis spectra of Mn^{III}(salen)(Cl) from (*R*,*R*)-**2** (black line) and **2**-N_3 (red line) in CH_2Cl_2 (0.3 mM) at 233 K. (b) Circular dichroism spectra of Mn^{III}(salen)(Cl) from (*R*,*R*)-**2** (black line) and **2**-N_3 (red line) in CH_2Cl_2 (0.3 mM) at 233 K.

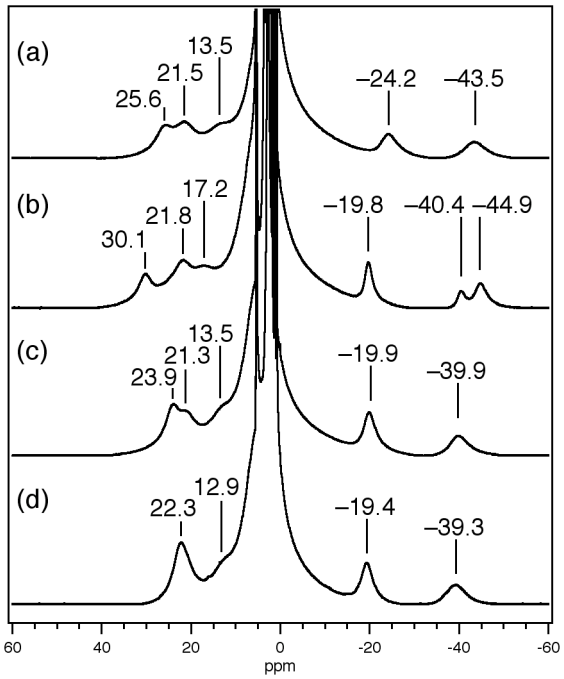

Figure S6. ^{1}H NMR (500 MHz) spectra of (a) **1**-Cl, (b) **1**-NO_3, (c) **1**-N_3. and (d) **1**-OCH_2CF_3 in CD_2Cl_2 (20 mM) at 233 K.

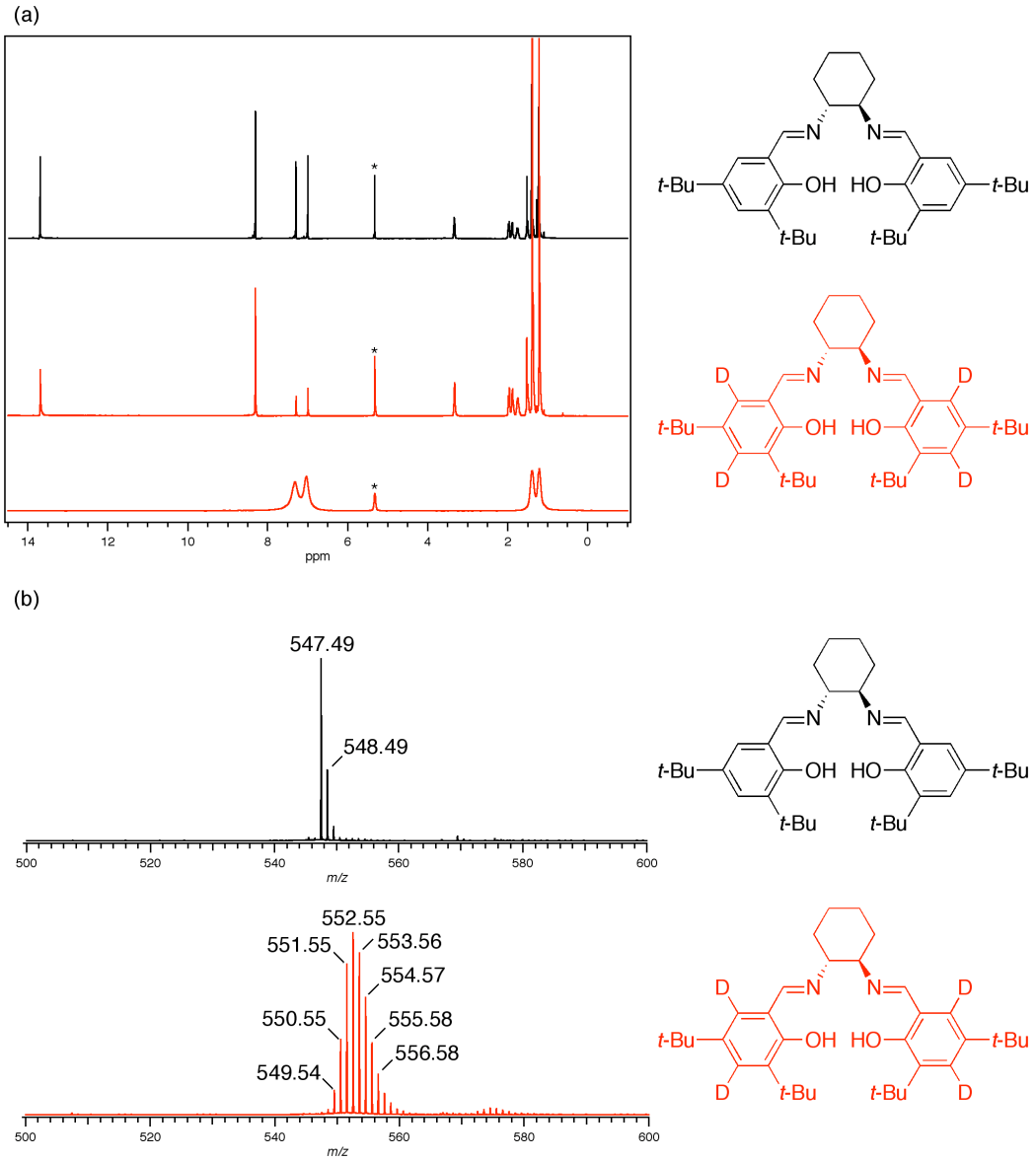

Figure S7. (a) ^{1}H NMR (500 MHz) spectra of (*R*,*R*)-**1** (top) and (*R*,*R*)-**1**-*d* (middle) in CD_2Cl_2 (20 mM) in comparison with the ^{2}H NMR (76.65 MHz) spectrum of (*R*,*R*)-**1**-*d* in CH_2Cl_2 (20 mM) at 298 K (bottom). The signal designated with an asterisk comes from residual $CHDCl_2$. (b) ESI-MS spectra of (*R*,*R*)-**1** (top) and (*R*,*R*)-**1**-*d* (bottom) in CH_3OH containing 0.01% of CF_3CO_2H at the cone voltage of 30 V.

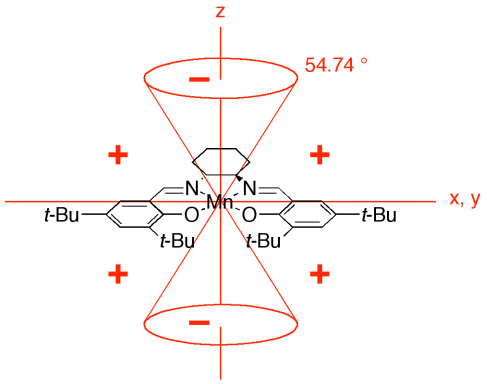

Figure S8. Schematic illustration of dipolar shifts with respect to the angle between the shifted nucleus and the z axis. Dipolar shifts reach 0 on the cone at the angle of 54.74 °, and increase with deviation from this cone. See, for details: Ming, L.-J. In *Physical Methods in Bioinorganic Chemistry, Spectroscopy and Magnetism*; Que, L., Jr., Ed.; University Science Books: California, 2000; p 375.

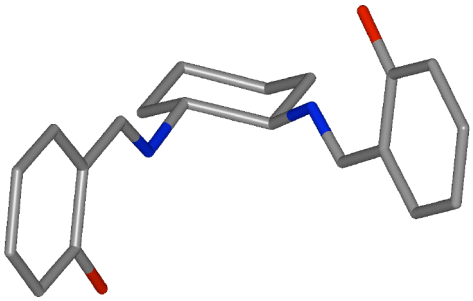

Figure S9. Optimized geometry of the salen ligand model with a DFT calculation at the B3LYP/6-311+G(d) level of theory.

Table S1. Assignment of the transitions that are Responsible for the CD from the Salen Ligand[a]

symmetry	transition[b]	coefficient
1B	86 to 89	0.57669
1B	85 to 90	0.57085
1A	85 to 89	0.56474
1A	86 to 90	0.56221
2A	82 to 89	–0.60287
2A	81 to 90	0.50399
2B	82 to 90	0.57673
2B	81 to 89	–0.53818
3B	84 to 89	0.51518
3B	83 to 90	–0.48000
3A	83 to 89	–0.43898
3A	84 to 90	0.42921

[a] An optimized structure of the salen ligand with a DFT calculation, for which SAC-CI calculations are carried out, is shown in Figure S9.. [b] Molecular orbitals are shown in Figure S10.

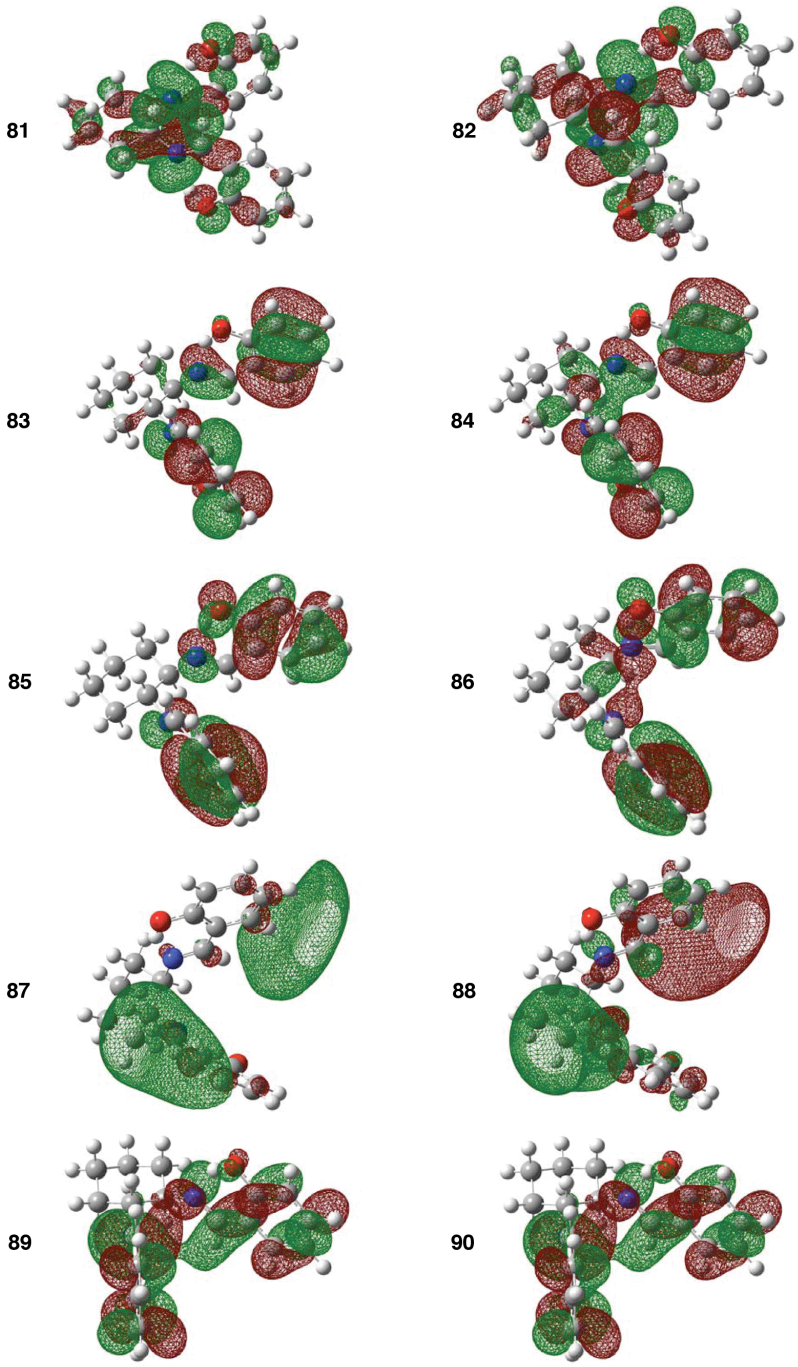

Figure S10. Molecular orbitals that are responsible for the CD from the salen ligand. The numbers designate the molecular orbitals shown in Table S1.

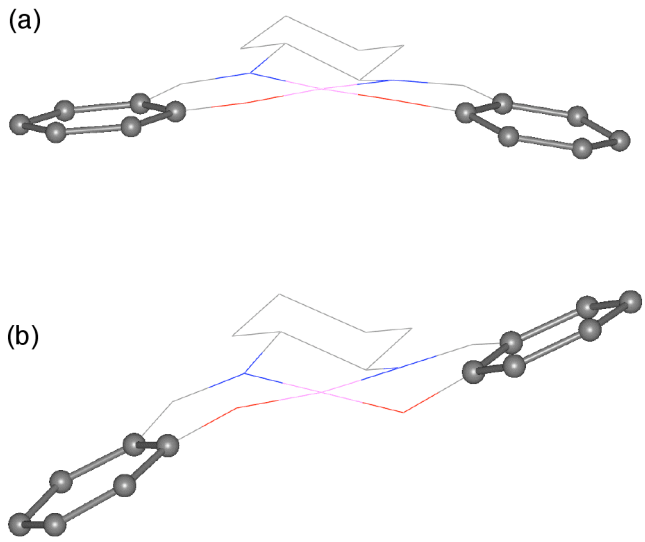

Figure S11. Hypothetical structures for quantum chemical calculations, which are depicted in a ball and stick model without hydrogen atoms. Structures in (a) and (b) are created from **1**-Cl and **1**-OCH_2CF_3, respectively.

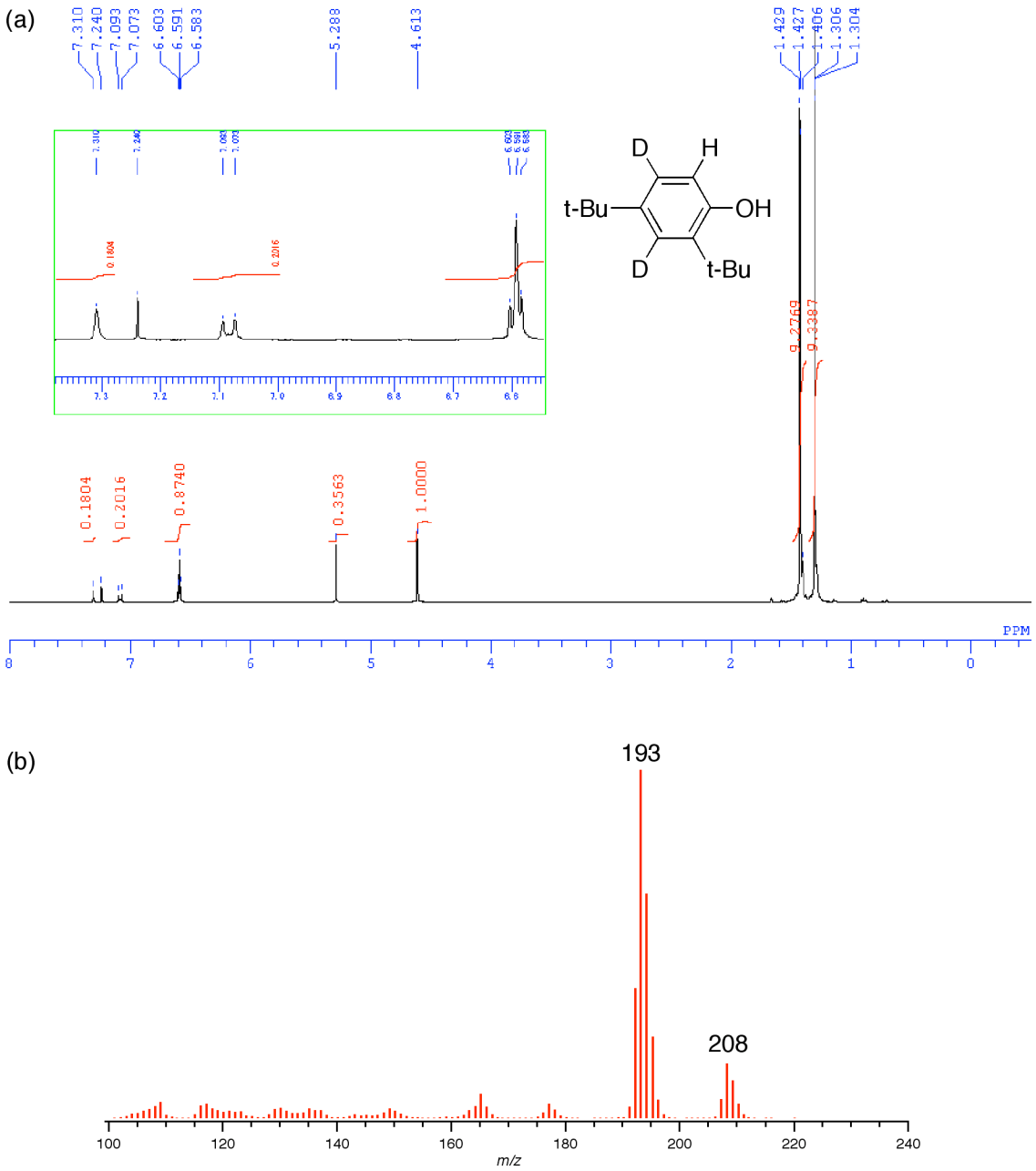

Figure S12. (a) ^{1}H NMR (400 MHz) spectrum of 2,4-di-*tert*-butylphenol-*d* in $CDCl_3$. The signal at 5.288 comes from CH_2Cl_2 that is utilized for column chromatography. (b) EI-MS spectrum of 2,4-di-*tert*-butylphenol-*d*.

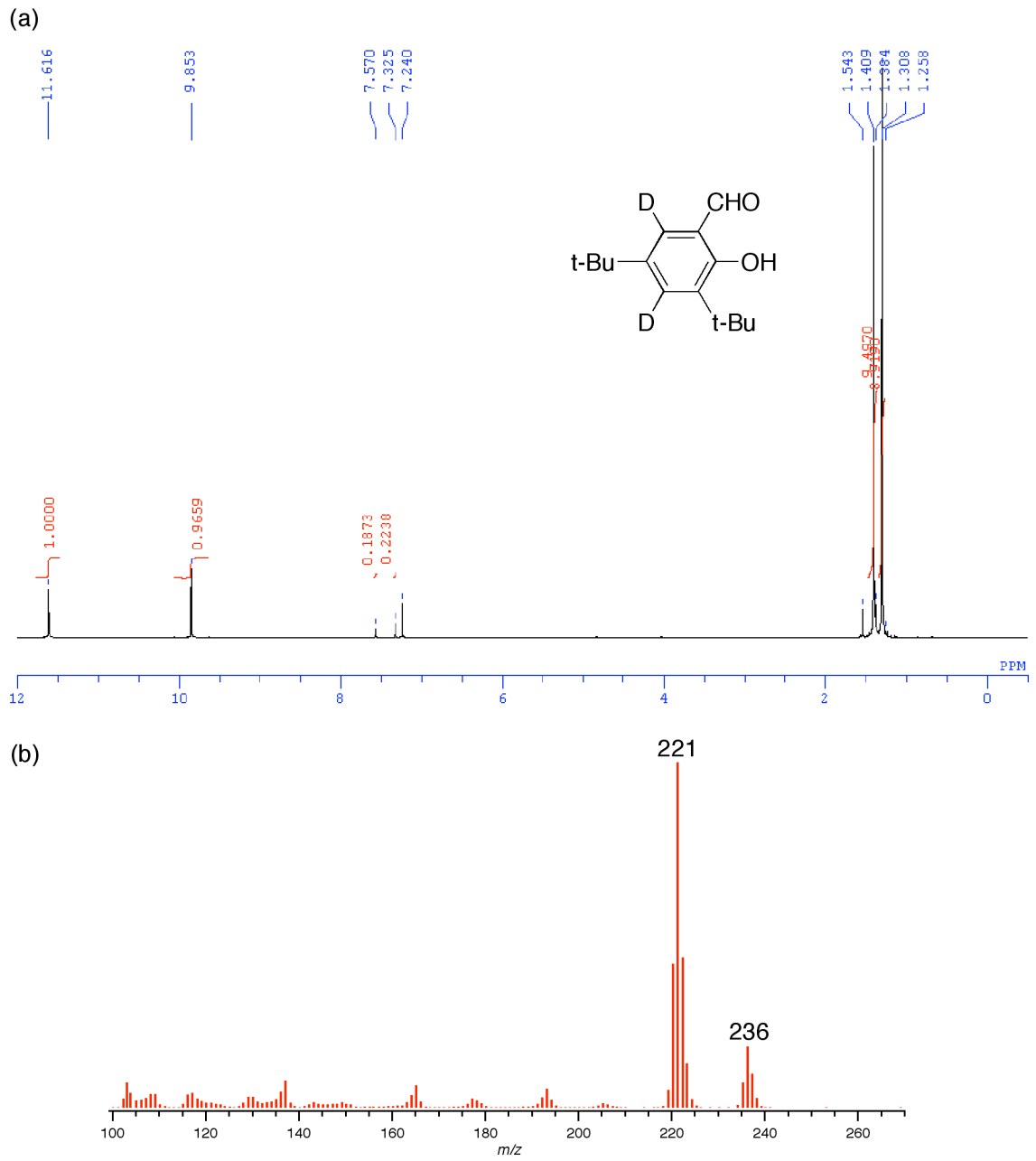

Figure S13. (a) ^{1}H NMR (400 MHz) spectrum of 3,5-di-*tert*-butyl-2-hydroxybenzaldehyde-*d* in $CDCl_3$. (b) EI-MS spectrum of 3,5-di-*tert*-butyl-2-hydroxybenzaldehyde-*d*.

(41) Frisch, M. J.; Trucks, G. W.; Schlegel, H. B.; Scuseria, G. E.; Robb, M. A.; Cheeseman, J. R.; Montgomery, J. A., Jr.; Vreven, T.; Kudin, K. N.; Burant, J. C.; Millam, J. M.; Iyengar, S. S.; Tomasi, J.; Barone, V.; Mennucci, B.; Cossi, M.; Scalmani, G.; Rega, N.; Petersson, G. A.; Nakatsuji, H.; Hada, M.; Ehara, M.; Toyota, K.; Fukuda, R.; Hasegawa, J.; Ishida, M.; Nakajima, T.; Honda, Y.; Kitao, O.; Nakai, H.; Klene, M.; Li, Raghavachari, K.; Foresman, J. B.; Ortiz, J. V.; Cui, Q.; Baboul, A. G.; Clifford, S.; Cioslowski, J.; Stefanov, B. B.; Liu, G.; Liashenko, A.; Piskorz, P.; Komaromi, I.; Martin, R. L.; Fox, D. J.; Keith, T.; Al-Laham, M. A.; Peng, C. Y.; Nanayakkara, A.; Challacombe, M.; Gill, P. M. W.; Johnson, B.; Chen, W.; Wong, M. W.; Gonzalez, C.; Pople, J. A. *Gaussian03*, revision C.03; Gaussian, Inc.: Pittsburgh, PA, 2004.